Available online at www.sciencedirect.com
SCIENCE DIRECT®
International Journal of Thermal Sciences 43 (2004) 809–816
International Journal of Thermal Sciences
www.elsevier.com/locate/ijts

Alternative models for transient convection heat transfer in external flows over a plate exposed to a variable heat flux

Mohammed Lachi [a,*], Mourad Rebay [a], Emilia Cerna Mladin [b], Jacques Padet [a]

[a] *Laboratoire de thermomécanique, UTAP, faculté des sciences, BP 1039, 51687 Reims, France*
[b] *Département de génie mécanique, université polytechnique, 313, S. Independentei, 77206 Bucarest, Romania*

Received 20 August 2003; received in revised form 10 February 2004; accepted 24 February 2004

Available online 9 June 2004

Abstract

Most of the existing studies and derived correlations relate to a uniform and constant heat flux or temperature imposed on a solid surface on which a parallel flow is developed. More recent works deal with unsteady forced convection over a flat plate when the boundary conditions change in the time. The present study presents a mathematical model of the unsteady convective heat transfer when the heat flux density is variable in time. Based on the energy equation formulation, this allows the analysis of the heat transfer characteristics associated with a constant laminar parallel flow over a negligible thickness plate. Transients are induced by two heat flux step changes imposed on the plate surface. The modelling approach is based on two methods: the integral method where a fourth order Karman–Pohlhausen polynomials are used for velocity and temperature profiles within the boundary layers, and the differential method with similarity solution. The purpose of this work is to provide new insights into unsteady convection modelling. In addition, we meant to draw attention to some discordance between the temporal evolution of the dimensionless parameters and the physical ones.

Keywords: Transient convection heat transfer; External forced convection; Unsteady convection; Integral method; Differential method; Convective heat transfer coefficient

1. Introduction

Convection heat transfer is a complex energy transport mechanism, as it involves fluid motion as well as heat diffusion. Therefore, in practical applications, the resolution of a heat transfer problem between a fluid and a solid often requires the knowledge of the heat transfer coefficient, usually denoted by "h". This coefficient incorporates flow features and thermal properties of both fluid and solid. It was introduced by the cooling law of Newton, expressed for steady regimes as: $\phi = h(T_p - T_f)$. In the absence of complementary data, there is a trend to extrapolate this expression to transient regimes as well. But, in many cases, when the boundary conditions are time-dependent, this formulation seems to be inadequate and an unsteady approach is needed.

An alternative approach to solving the boundary layer equations in the external convective heat transfer involves the use of one of these three techniques: integral, differential or purely numerical method. The integral approach was originally proposed by von Karman and applied by Pohlhausen [1], thus avoiding the inherent complications associated with similarity methods. The procedure implies first assuming polynomial profiles for the unknown U and T, and then resolution of the boundary layer integral momentum and energy equations in a dimensional form [2–8] in cases of steady and unsteady state problem. The differential method leads to a similarity solution [9–11] by use of appropriate dimensionless groups; this approach reduces the partial differential energy equation to an ordinary differential equation. The purely numerical method is used especially to solve the complex problems associated with a particular geometry.

The use of dimensionless numbers is a common practice to nondimentionalize the heat transfer coefficient and to compress the representation of results. In such cases, the description of the convective transport phenomena may

* Corresponding author.
E-mail address: m.lachi@univ-reims.fr (M. Lachi).

1290-0729/$ – see front matter
doi:10.1016/j.ijthermalsci.2004.02.021

Nomenclature

a	thermal diffusivity	$m^2 \cdot s^{-1}$	
C	constant		
h	convective heat transfer coefficient	$W \cdot m^{-2} \cdot K^{-1}$	
Nu	Nusselt number		
Pr	Prandtl number		
Sr_x	Strouhal number		
t	time variable	s	
T	fluid temperature	K	
U	velocity component parallel to the plate	$m \cdot s^{-1}$	
V	velocity component perpendicular to the plate	$m \cdot s^{-1}$	
x, y	Cartesian co-ordinates	m	

Greek symbols

δ	dynamical boundary layer thickness	m
δ_t	thermal boundary layer thickness	m
η	dynamic similarity variable	
ϕ	heat flux density	$W \cdot m^{-2}$
λ	thermal conductivity	$W \cdot m^{-1} \cdot K^{-1}$
ν	kinematic viscosity	$m^2 \cdot s^{-1}$
θ	temperature difference $(T - T_\infty)$	K

Superscripts

$'$	differentiation with respect to η
$*$	dimensionless temperature
$+$	dimensionless quantities

Subscripts

f	related to the fluid
p	related to the plate surface $(y = 0)$
∞	in the free stream (at infinity)

sometimes lead to wrong interpretations [12]. The present work will emphasize this aspect, by considering the transient thermal interaction between a laminar boundary layer flow and a semi-infinite flat plate. The unsteady system behaviour is entirely due to the generation of an impulsive heat flux step change on the upper face of the flat surface.

This work provides new data on the unsteady behaviour of the heat exchange coefficient, in addition to other previous theoretical [4–8,16] and experimental [13–15] (e.g., by using the flash method) studies. Moreover, the results are useful in engineering applications where a transient boundary condition and a thin contact surface are encountered.

2. Description of the problem

We consider a laminar steady parallel fluid flow over a zero-thickness semi-infinite flat plate, initially at thermal equilibrium. The fluid is assumed to have a Prandtl number $= 0.7$, such as the thermal boundary layer is thinner than the hydrodynamical one. The velocity and temperature values of the incident flow are respectively U_∞ and T_∞. The thermophysical properties are assumed to be constant, such as the fluid hydrodynamical boundary layer is independent of the temperature field. Initially, the plate temperature is assumed to be at the same temperature as the fluid, T_∞. For times $t \geqslant 0$, the plate surface $(y = 0)$ is subjected to a time dependent heat flux density $\phi(t)$ which consists of two uniform step changes: from 0 to ϕ_1 and from ϕ_1 to ϕ_2. Time t_1 is the duration of the first step, while ϕ_2 is applied indefinitely after this duration, as illustrated in Fig. 1. The plate has a negligible thickness and is absolutely insulated at the bottom. As a result, the applied heat flux is fully reflected towards the fluid. The schematic representation of the problem is shown in Fig. 1.

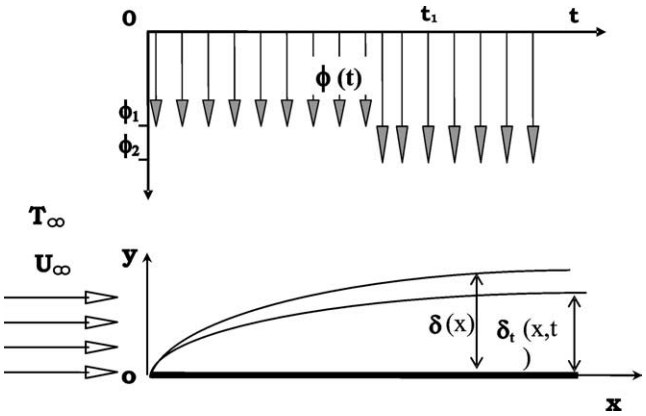

Fig. 1. Description of the problem.

3. Governing equations

Under steady-state flow but transient heat transfer conditions, the mass, momentum and energy conservation equations are given by:

$$\frac{\partial U}{\partial x} + \frac{\partial V}{\partial y} = 0 \tag{1}$$

$$U\frac{\partial U}{\partial x} + V\frac{\partial U}{\partial y} = \nu\frac{\partial^2 U}{\partial y^2} \tag{2}$$

$$\frac{\partial T}{\partial t} + U\frac{\partial T}{\partial x} + V\frac{\partial T}{\partial y} = a_f\frac{\partial^2 T}{\partial y^2} \tag{3}$$

The initial time and boundary conditions to be satisfied by the velocity and temperature profiles within the fluid are as follows:

$$\left.\begin{aligned} &T = T_\infty \quad \text{at } t = 0 \\ &-\lambda_f\left(\frac{\partial T}{\partial y}\right)_{y=0} = \phi(t) \\ &\quad = \begin{cases} \phi_1 & \text{for } 0 < t \leqslant t_1 \\ \phi_2 & \text{for } t > t_1 \end{cases} \end{aligned}\right\} \quad \text{at } x > 0,\ y = 0 \tag{4}$$

$$U = U_\infty, \quad T = T_\infty \quad \text{at } x = 0,\ y > 0$$
$$U = 0, \quad V = 0 \quad \text{at } x > 0,\ y = 0$$
$$U = U_\infty \quad \text{at } x > 0,\ y \geqslant \delta$$
$$T = T_\infty \quad \text{at } x > 0,\ y = \delta_t$$
$$T = T_p(x,t) \quad \text{at } x > 0,\ y = 0 \tag{5}$$

The following temperature differences are defined for convenience:

$$\theta = (T - T_\infty) \quad \text{and} \quad \theta_p = (T_p - T_\infty)$$

The problem can be represented by the time dependent semi-integral form of the energy equation, written in dimensionless form as:

$$\frac{\partial}{\partial t}\int_0^{\delta_t} \theta \,\mathrm{d}y + \frac{\partial}{\partial x}\int_0^{\delta_t} U\theta \,\mathrm{d}y = -a_f \frac{\partial \theta}{\partial y}\Big|_{y=0} \tag{6}$$

The solution methodology applied to Eq. (6) is based on the 4-order polynomial Karman–Pohlhausen approach for both velocity and temperature fields.

With the foregoing conditions given by Eq. (5), the temperature profile results as the following fourth-order polynomial:

$$\theta = \theta_P\Big[1 - 2\frac{y}{\delta_t} + 2\left(\frac{y}{\delta_t}\right)^3 - \left(\frac{y}{\delta_t}\right)^4\Big] \tag{7}$$

In a similar manner, the velocity profile is modelled by:

$$U = U_\infty\left[2\frac{y}{\delta} - 2\left(\frac{y}{\delta}\right)^3 + \left(\frac{y}{\delta}\right)^4\right]$$
$$\text{where } \delta = \frac{5.83x}{\sqrt{Re_x}} = C\sqrt{x} \tag{8}$$

The thermal boundary layer thickness is obtained from Eq. (4), where the temperature gradient at the surface is calculated by Eq. (7):

$$\delta_t(x,t) = 2\lambda_f \frac{\theta_P(x,t)}{\phi(t)} \tag{9}$$

By substituting Eqs. (7)–(9) into Eq. (6), the following partial differential equation is obtained for the surface temperature θ_p:

$$\left(\frac{8U_\infty}{5\lambda_f^2}x^{-1/2}\phi^3\theta_P^2 - \frac{12U_\infty}{7C^3}x^{-3/2}\phi\theta_P^4 + \frac{16\lambda_f U_\infty}{15C^3}x^{-2}\theta_P^5\right)\frac{\partial\theta_P}{\partial x} + \frac{6C}{5\lambda_f^3}\phi^4\theta_P\frac{\partial\theta_P}{\partial t} - \frac{3C}{5\lambda_f^3}\phi^3\theta_P^2\frac{\partial\phi}{\partial t} - \frac{4U_\infty}{15\lambda_f^2}x^{-3/2}\phi^3\theta_P^3 + \frac{18U_\infty}{35C^2}x^{-5/2}\phi\theta_P^5 - \frac{16\lambda_f U_\infty}{45C^3}x^{-3}\theta_P^6 = \frac{a_f C}{\lambda_f^5}\phi^6 \tag{10}$$

It should be noted that, for no time-variation in the heat flux, the derivative $\frac{\partial\phi}{\partial t}$ is equal to zero in Eq. (10). For any other imposed function $\phi(t)$, the foregoing equation may be numerically integrated to lead to a solution for $\theta_p(x,t)$.

In this study, we will consider as reference case the system with air as fluid and a flow velocity of $U_\infty = 1\ \mathrm{m{\cdot}s^{-1}}$. Initially (at $t = 0$) the temperature of the system is T_∞.

Two cases of step changes in the surface heat flux density $\phi(t)$, from an initial isothermal state, are studied here.

Form A: the first stage is due to the variation of the heat flux density from 0 to $\phi_1 = 10\ \mathrm{W{\cdot}m^{-2}}$ and the second is associated to the step change from ϕ_1 to $\phi_2 = 100\ \mathrm{W{\cdot}m^{-2}}$ (overheating).

Form B: the first stage is due to the variation of the heat flux density from 0 to $\phi_1 = 100\ \mathrm{W{\cdot}m^{-2}}$ and the second is associated to the step change from ϕ_1 to $\phi_2 = 10\ \mathrm{W{\cdot}m^{-2}}$ (relaxation).

In both cases the time duration, of the first step from 0 to ϕ_1, is fixed at $t_1 = 0.3$ s, and ϕ_2 is applied for all times over this duration.

With the knowledge of the surface temperature $\theta_p(x,t)$ and the applied surface heat flux, the transient convective heat transfer coefficient h and local Nusselt number Nu can be determined

$$h(x,t) = \frac{\phi(t)}{\theta_p(x,t)} \tag{11}$$

$$Nu(x,t) = \frac{h(x,t)\cdot x}{\lambda_f} \tag{12}$$

4. Numerical resolution

Eq. (10) was solved by use of the finite difference method with an explicit upwind numerical scheme. The integration time step was constant and equal to $\Delta t = 0.005$ s, while the space step varied from $\Delta x = 2 \times 10^{-4}$ m near the plate leading edge, to $\Delta x = 10^{-3}$ m beyond the abscissa $x = 1$ cm.

Using the subscript j to denote time, and subscript i to represent the x location, the numerical representation used for the discretized Eq. (10) is given by:

$$A_6\theta^6_{P_{(i+1,j+1)}} + A_5\theta^5_{P_{(i+1,j+1)}} + A_4\theta^4_{P_{(i+1,j+1)}} + A_3\theta^3_{P_{(i+1,j+1)}} + A_2\theta^2_{P_{(i+1,j+1)}} + A_1\theta_{P_{(i+1,j+1)}} + A_0 = 0 \tag{13}$$

A computer Borland Turbo Pascal program was written to solve Eq. (13) for each mesh node $(i+1, j+1)$, by means of an iterative scanning process applied to the closed interval where positive roots exist. Such intervals are identified with the aid of the Sturm rule procedure [8]:

$$\text{Maximal limit} = 1 + \frac{1}{|A_0|}\max\{|A_i|\} \quad \text{and}$$
$$\text{Minimal limit} = \frac{|A_6|}{|A_6| + \max\{|A_i|\}} \tag{14}$$

After bracketing the root of the function (13) by (14) we use an hybrid algorithm taken Newton–Raphson and Bisection subroutine [17]. The root returned will be refined untill its accuracy is known witin $\pm 10^{-6}$.

5. The differential method

To validate the integral method, the same problem was resolved by a differential method [10], applied after the initial partial differential system Eqs. (1), (2) and (3) as transformed into ordinary differential equations.

By introduction of the similarity variable

$$\eta = \frac{y}{\sqrt{\nu x / U_\infty}} \tag{15}$$

In the momentum conservation Eq. (2), the velocity components in the x and y directions become

$$U = U_\infty F'(\eta), \qquad V = \frac{1}{2}\sqrt{\frac{\nu U_\infty}{x}}\left(\eta F' - F\right) \tag{16}$$

They verify the well-known Blasius equation given by:

$$F''' + \frac{1}{2} F F' = 0 \tag{17}$$

With the dynamic boundary conditions:

$$F'(\eta = 0) = 0, \qquad F'(\eta = \infty) = 1 \tag{18}$$

For the calculation of the unsteady temperature field the following dimensionless quantities are introduced:

$$t^+ = \frac{U_\infty t}{x} = Sr_x \tag{19}$$

$$T^* = T^*\left(\eta, t^+\right) = \frac{\theta}{\theta_p} \tag{20}$$

where Sr_x is the Strouhal number.

It is shown in [10] that the similarity solutions in the form (20) exist only if

$$\begin{cases} \theta = \frac{\phi(t)}{\lambda_f}\sqrt{\frac{\nu x}{U_\infty}} G\left(\eta, t^+\right) \\ \theta_p = \frac{\phi(t)}{\lambda_f}\sqrt{\frac{\nu x}{U_\infty}} G\left(0, t^+\right) \end{cases} \tag{21}$$

By these transformations, the dimensionless temperature $G(\eta, t^+)$ is obtained from the partial differential equation:

$$\frac{1}{Pr} G'' - \frac{1}{2} F' G + \frac{1}{2} F G' = \left[1 - F' t^+\right]\left(\frac{\partial G}{\partial t^+}\right) \tag{22}$$

with the initial and boundary conditions:

$$\begin{aligned} &0 < t^+ \leqslant t_1^+ \colon\ G'\left(0, t^+\right) = -1 \\ &t_1^+ < t^+ \leqslant \infty \colon\ G'\left(0, t^+\right) = -\frac{\phi_2}{\phi_1} \\ &0 < t^+ \leqslant \infty \colon\ G\left(\infty, t^+\right) = 0 \end{aligned} \tag{23}$$

Numerical resolution of the transient differential equation (22) is obtained by a combination of two types of finite differences schemes: an implicit one when the temporal coefficient $(1 - F' t^+)$ is positive (for the grid points near the plate, where $F' \ll 1$) and an explicit one in the negative case. Then, the values of G are calculated for each grid points (η, t^+) in the dimensionless space, especially the non-dimensional surface temperature $G(0, t^+)$ from which the convective heat transfer coefficient is deduced.

6. Results and discussion

6.1. Time evolutions by the Karman–Pohlhausen method

The interface temperature, the convective heat transfer coefficient and the Nusselt number responses obtained are plotted, respectively, in Figs. 2, 3 and 4 for the first case (form A), and in Figs. 5, 6 and 7 for the second one (form B). Remarkable are the highly unsteady behaviour of these parameters, as illustrated by the graphs.

For the temperature curves, it appears that, in both cases, the steady state solution is reached at a very short time of about 0.28 s from the leading edge of the plate to the location $x = 10$ cm. This result agrees with the value given by [8]. For the locations over $x = 10$ cm, they reach their steady state values in the second stage of the heat flux step change.

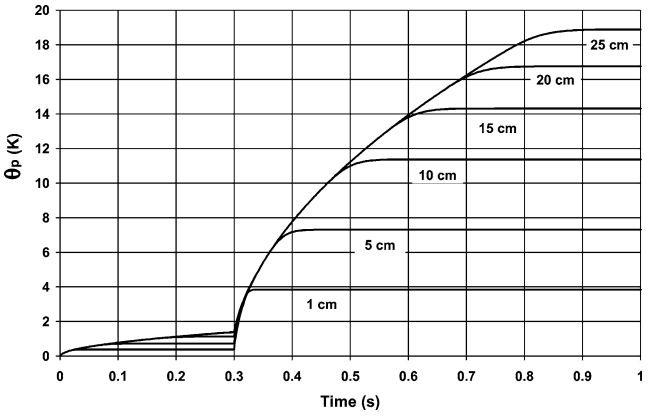

Fig. 2. Surface temperature responses in the firt case of heat step change density (form A).

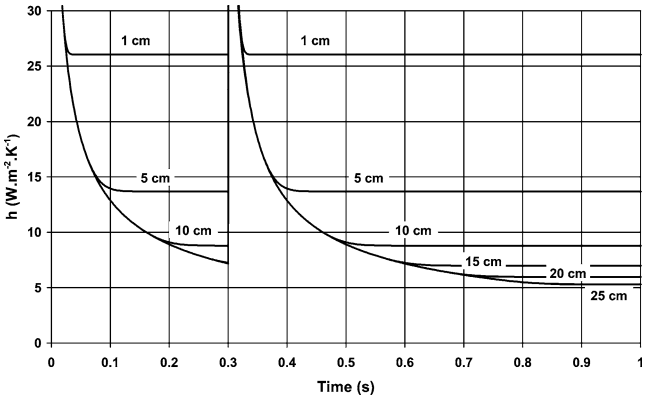

Fig. 3. Transient convective heat transfer coefficient, at different locations x, in the first case.

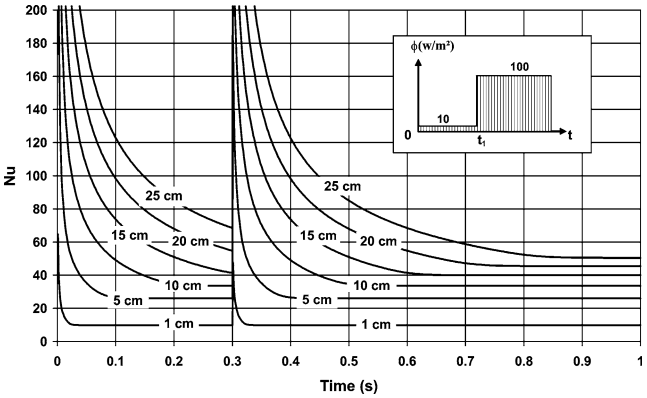

Fig. 4. Transient local Nusselt number, *Nu*, with time, t, at different locations x, in the first case.

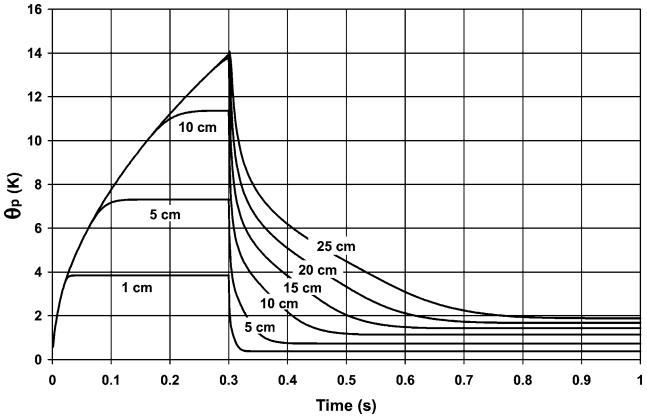

Fig. 5. Surface temperature responses to the second heat flux step change (form B).

Temperature curves of both cases present a good agreement with the steady state solution (15) of Karman–Pohlhausen [16], when increasing the time and the abscissa.

$$\theta_p(x) = \frac{\phi}{0.447\lambda_f Pr^{1/3}}\sqrt{\frac{\nu x}{U_\infty}} \tag{24}$$

For the beginning of the unsteady process due to the first step change, the evolution of the temperature, for all locations, merge, and this indicates that the first stage of this type of heat exchange is purely a conductive phenomena. A singular point appears at time $t_1 = 0.3$ s, where the heat flux step changes its value. Thus, we observe two distinctive behaviours according to the form of the heat flux step change in the second stage evolution when $t > t_1$. For the first case, when ϕ_2 is greater than ϕ_1, an overheating phenomenon appears. Therefore, the surface temperature increases significantly and reaches steady state values that depend on the location x. As in the beginning of the first step change, during the first times of this second stage the heat transfer is also conductive. Meanwhile, for the second case (form B), when ϕ_2 is less than ϕ_1, a relaxation phenomena appears and therefore, the surface temperature decreases slowly in time and tends to the steady state values. As a result, the plate temperature field has smaller values than during the first stage.

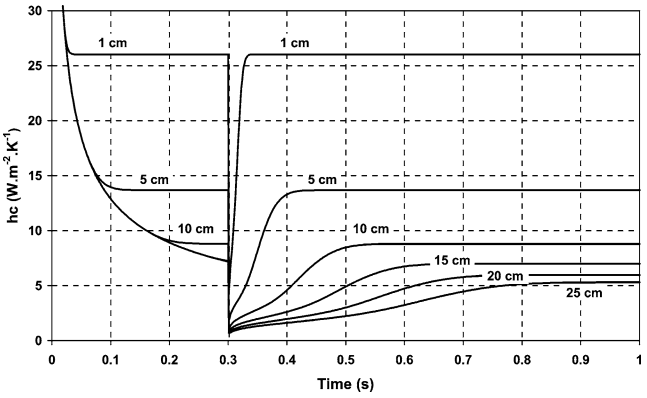

Fig. 6. Transient convective heat transfer coefficient, at different locations x, in the second case.

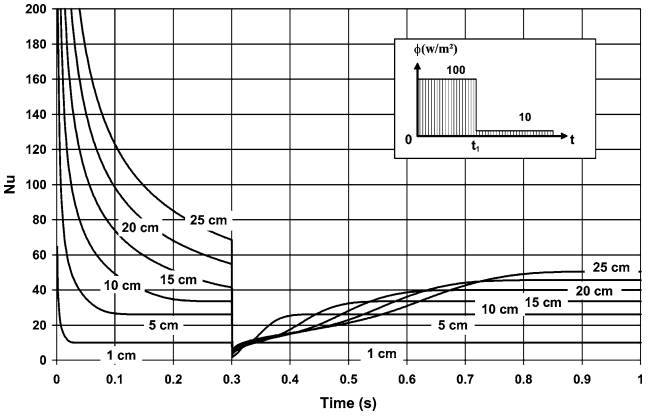

Fig. 7. Transient local Nusselt number, *Nu*, with time, t, at different locations x, in the second case.

It is seen that for both step changes the temperature is higher as the value of the heat flux step is the greater one. This results from the fact that the plate thickness is neglected and has no thermal capacity.

In Figs. 3 and 6 it can be seen the dependence of the convective heat transfer coefficient on the abscissa x along the plate, it increases with x from 1 to 25 cm. In the first stage, where $0 < t < t_1$, from an infinite value the convective heat transfer coefficient decreases rapidly. As we can see in the second stage, the distortions of the surface temperature induced by the step change in the heat flux form have repercussions on the convective heat transfer coefficient. Then, the lasts evolve in the same manner as in the first stage for the overheating case (Fig. 3), but in a completely different way for the relaxation case (Fig. 6) with form B. In the last case, the local convective heat transfer coefficient grows slowly until the steady state value, from an initial value as little as the location x is at far distance from the plate entrance.

In industry, instead of the convective heat transfer coefficient, the Nusselt number *Nu* is usually used in the convection calculations, so it is interesting to present some tran-

sient Nusselt number predictions. These are shown in Figs. 4 and 7 where the transient Nusselt number, is graphed as a function of time, for different x locations. All Nusselt number curves begin at infinity at $t = 0$ and rapidly decrease with time before a period in which they slowly decrease and then tend towards the steady state value. As seen in these figures, the distortions of the *Nu* number appear after the application of the second step change from ϕ_1 to ϕ_2. For the form A of the heat flux density, during the transient evolution, the *Nu* number is as higher as the abscissa x is a greater one. For the form B, contrary to the responses to the first form A of the heat flux density, *Nu* number for the first abscissa (i.e., $x = 5$ cm) can be greater than the *Nu* corresponding to the locations at far distances from the plate (e.g., $x = 25$ cm). Nevertheless, under steady state conditions, *Nu* increases with increasing x.

6.2. Comparison with the differential method

The evolutions of the non-dimensional surface temperature $G(0, t^+)$, calculated at five abscissa x: 5, 10, 15, 20 and 25 cm from the leading edge of the plate, are plotted in the Figs. 8 and 9, respectively, for the form A and for the form B step change. In the first stage, due to the first step change ϕ_1 from an initial isothermal state at $t^+ = 0$, the dimensionless temperature evolutions are similar for all abscissa x. Whereas, they are not similar on all abscissa x in the second stage evolution, due to the step change from ϕ_1 to ϕ_2. Indeed, the beginning of the second stage in the dimensionless time (t^+) depends on the location x. This time is equal to t_1^+ and corresponds, at each abscissa x, to $t_1 = 0.3$ s (see Eq. (19)). In addition, the dimensionless temperature tends, at each abscissa x, to the same constant value corresponding to the steady state.

From the evolutions of the dimensionless surface temperature $G(0, t^+)$ one can deduce the dimensional ones in time from Eq. (21). These dimensional temperature evolutions $\theta_p(x, t)$ are given for the two forms of step changes in Figs. 10 and 11.

The dimensional surface temperatures obtained by the differential method differ slowly from those derived from the integral method and are given in Figs. 2 and 5. The difference is less than 7%, as it can be seen in Fig. 12, and is essentially due to the choice of velocity and temperature profiles used in the integral method. Indeed, the forth order polynomial profiles chosen here give the steady state

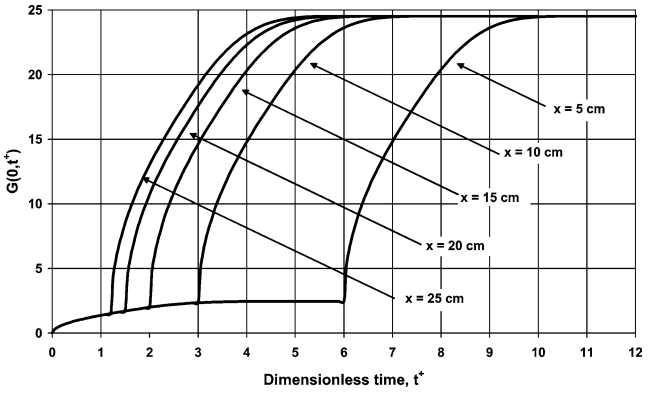

Fig. 8. Non-dimensional surface temperature responses to the first heat flux step change (form A).

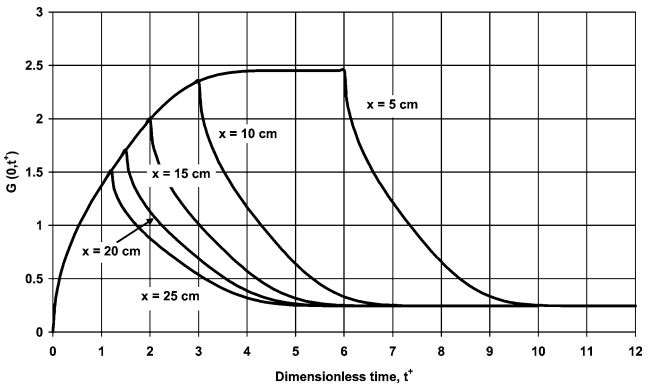

Fig. 9. Non-dimensional surface temperature responses to the second heat flux step change density (form B).

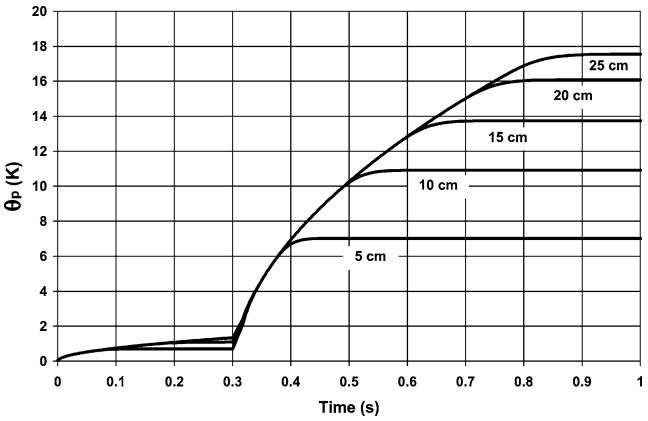

Fig. 10. Surface temperature responses to the first heat flux step change (form A).

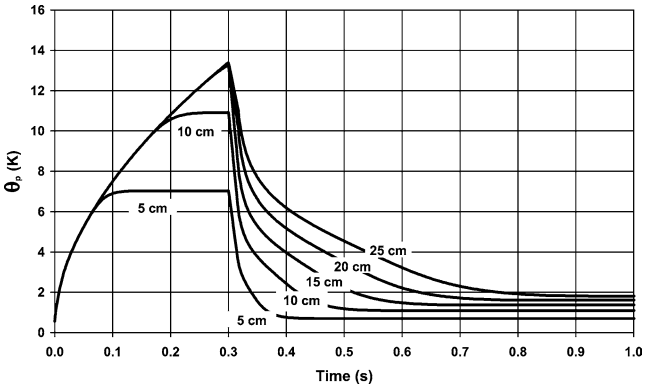

Fig. 11. Surface temperature responses to the second heat flux step change (form B).

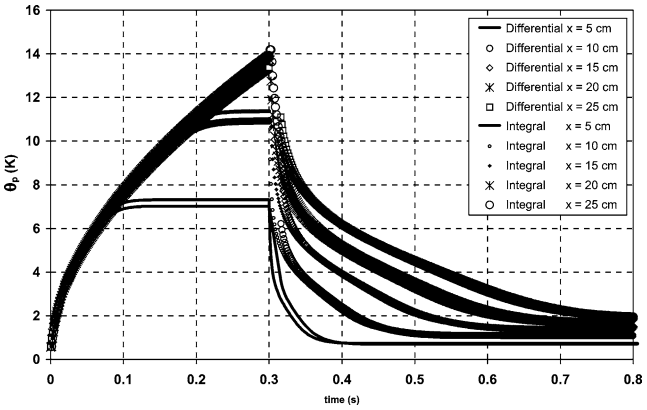

Fig. 12. Difference between the results of the differential and the integral approaches on the temperature responses.

temperature (Eq. (15)) different from that obtained by the differential method [16]:

$$\theta_p(x) = \frac{\phi}{0.46\lambda_f Pr^{1/3}}\sqrt{\frac{\nu x}{U_\infty}} \tag{25}$$

The difference between the steady state surface temperatures obtained by the integral method (Eq. (15)) and by the differential method (Eq. (24)) is reflected in the denominator coefficient, which is 0.447 in the first equation and 0.46 in the second one. Different polynomial profiles have been tested in the integral method, but they lead to greater differences compared to the differential method results.

6.3. From the dimensionless results to the physical ones

Through the integral method, the Nusselt number (non-dimensional parameter) is derived from the convective heat transfer coefficient, which is a dimensional parameter. By the differential method, the dimensional surface temperatures, from which the convective heat transfer coefficient is calculated, are deduced from the dimensionless ones $G(0, t^+)$.

As it was mentioned above, there are some disagreements between the time evolution behaviors of the non-dimensional parameters and the physical results, especially during the relaxation process. In fact, without some care, one can deduce from the evolution of the local *Nu* number given in Fig. 7, that during the relaxation phase the heat exchange is less pronounced near the plate leading edge than farther. By contrast, the convective heat transfer coefficient evolution (Fig. 6) shows that the inverse behaviour is physically true. In order to not distort the physical meaning of numerical solutions, great care must be taken in choosing the dimensionless parameters. For instance, a local Nusselt number as defined by Eq. (12) is meaningless since it contains two variables, h and x, with opposite variations (i.e., h decreases with increasing x).

Attention is also drawn to the evolutions of the non-dimensional temperature $G(0, t^+)$ in Figs. 8 and 9. They show that, at any abscissa x, this parameter varies and reaches a unique value associated with the steady state. While, the physical representations of the surface temperature in Figs. 2 and 5 indicate that the steady state values depend on the location x.

In conclusion, the return to the dimensional results, expressed in terms of physical parameters, is essential to well understand the physical problems, especially for the engineer who must work in the real space. Although the use of the dimensionless numbers is a convenient way of compressing data, but the description of the transport phenomena in non-dimensional space can induce some incorrect interpretations and conclusions if the non-dimensional parameters are not well defined or understood. In addition, the return to the physical parameter representation may point out some phenomena that are not evident in the non-dimensional results.

7. Conclusions

An analytical/numerical approximate solution has been presented for the laminar forced convection problem with a time variation in the heat flux density over a flat plat. A differential method based on exact similarity transformations was employed to validate the approximate integral method.

The highly unsteady behaviour of the surface temperature and the convective heat transfer coefficient is clearly put into evidence. These parameters are strongly dependent on the form of the boundary condition, especially during the transient regime. In addition, the asymptotic values show a good agreement with the steady state solutions.

As regards to the convective heat exchange coefficient, its evolution presents noticeably the same feature: from a very high value at the beginning of the transient regime, it decreases rapidly to reach a limiting value which is higher when the considered abscissa is nearer the leading edge of the plate.

However, some care must be taken when analysing the system evolution in non-dimensional space. In fact, the evolutions of the local Nusselt number present some discordance with those corresponding to the local convective heat transfer coefficient. These discordances are also noted when the dimensionless and the dimensional surface temperature are compared. By these exemples, we show that the return to the physical representation can bring some surprises and points out some phenomena not evident in the non-dimensional results. Then, to insure a correct interpretation of the physical phenomena, one should always return to a physical space with independent parameters.

References

[1] K. Pohlhausen, Z. Angew. Math. Mech. 1 (1921) 252.
[2] J. Sucec, Unsteady heat transfer between a fluid, with time varying temperature, and a plate: an exact solution, Internat. J. Heat Mass Transfer 18 (1975) 25–36.

[3] J. Padet, Principes des transferts convectifs, Polytechnica édition, Paris, 1997.
[4] G. Polidori, J. Padet, Transient forced convection with arbitrary variation in the wall heat flux, Heat Mass Transfer 38 (2002) 301–307.
[5] R. Wang, B. Chung, L. Thomas, Transient convective heat transfer for laminar boundary layer flow with effects of wall capacitance and resistance, J. Heat Transfer 99 (1977) 513–519.
[6] M. Lachi, G. Polidori, N. Chitou, J. Padet, Theoretical modelisation in transient convective heat transfer for laminar boundary layer flow, in: Proc. of International Centre for Heat and Mass Transfer, Turkey, 1996, pp. 27–36.
[7] B.T.F. Chung, S.A. Kassemi, Conjugate heat transfer for laminar flow over a plate with non steady temperature at the lower surface, J. Heat Transfer 102 (1980) 177–180.
[8] G. Polidori, M. Lachi, J. Padet, Unsteady convective heat transfer on a semi-infinite flat surface impulsively heated, Internat. Com. Heat Mass Transfer 25 (1) (1998) 33–42.
[9] S.R.C. Dennis, Unsteady Heat Transfer for Boundary-Layer Flow, Recent Research of Unsteady Boundary Layers, Laval University Press, Quebec, 1972.
[10] M. Rebay, J. Padet, Laminar boundary-layer flow over a semi-infinite plate impulsively heated or cooled, European Phys. J. Appl. Phys. 7 (1999) 263–269.
[11] M. Rebay, M. Lachi, J. Padet, Transient forced convection due to a positive step change on thermal wall conditions, Internat. J. Fluid Mech. Res. 27 (2000) 468–480.
[12] J. Padet, T. De Lorenzo, Similitude criteria for the free convective heat and mass transfer, Internat. J. Energy Res. 26 (2002) 365–381.
[13] D. Petit, J. Dard, A. Dégiovanni, Détermination du coefficient d'échange entre un fluide et une paroi, Rev. Gen. Therm. 238 (1981) 719.
[14] P. Pierson, J. Padet, Evaluation des transferts thermoconvectifs en régime instationnaire. Approche théorique et expérimentale, Rev. Gen. Therm. 287 (1985) 781.
[15] B. Remy, A. Degiovanni, D. Maillet, Mesure de coefficient d'échange pour des écoulements à faible vitesse, Rev. Gen. Therm. (1995) 28–42.
[16] G. Polidori, M. Rebay, J. Padet, Retour sur les résultats de la théorie de la convection forcée laminaire établie en écoulement de couche limite externe 2D, Internat. J. Therm. Sci. (1999) 398–409.
[17] W.H. Press, B.P. Flannery, S.A. Teukolsky, W.T. Vetterling, Numerical R. Books, Cambridge University Press, Cambridge, 1988–1992.